Ginkgo biloba extract 50 dropping pills improve vascular cognitive impairment through anti-oxidative and anti-inflammatory effects

FU-LING WANG[1-3], WEN-LAN LI[1,2] and HONG LI[3]

[1]School of Pharmacy, Harbin University of Commerce, Harbin, Heilongjiang 150076, P.R. China; [2]Postdoctoral Research Station of Chinese Materia Medica, Harbin University of Commerce, Harbin, Heilongjiang 150076, P.R. China; [3]Research Institute, Zhejiang Shangyao Jiuxu Pharmaceutical Co., Ltd., Jinhua, Zhejiang 321016, P.R. China

Received December 25, 2025; Accepted May 8, 2026

DOI: 10.3892/etm.2026.13210

Abstract. The aim of the present study was to investigate the improvement effect of *Ginkgo biloba* extract 50 dropping pill (GBE50DP) on vascular cognitive impairment (VCI) induced by cerebral ischemia and its mechanism. The VCI rat model was established by 2-vessel occlusion and randomly divided into the control, model, positive and GBE50DP administration groups. The administration groups were then administered GBE50DP intragastrically for 8 weeks. The social behavior and ability of learning and memory of each group were tested through the Morris water maze and eight-arm maze experiment. The content of oxidative stress and inflammatory factors in the hippocampus of rats were detected using ELISA. Hematoxylin & eosin staining and Terminal-deoxynucleotidyl transferase mediated nick end labeling staining were used to observe the morphological changes of nerve cells in the hippocampal CA1 region of rats. The expression of Caspase-3, Bcl-2, Bax, cytochrome *c* (Cyto-C), fibroblast-associated antigen (Fas) and poly(ADP-ribose) polymerase-1 (PARP-1) proteins in the hippocampal CA1 region of rats was detected by immunohistochemistry and western blot analysis. The blood components of GBE50DP were analyzed using liquid chromatography-tandem mass spectrometry. The model rats showed significant cognitive impairment; compared with the model group, in the GBE50DP administration groups, the social behavior of rats was markedly improved; the content of superoxide dismutase, glutathione peroxidase and catalase in the hippocampus was markedly increased and that of malondialdehyde, IL-1β, IL-6 and TNF-α was significantly decreased. The pathological changes and expression of Cyto-C, Bax, Bcl-2, Caspase-3, Fas and PARP-1 proteins in brain tissue were markedly improved. The index components of GBE50DP in blood included ginkgolide A, B, C and K and bilobalide, as well as flavonoids such as rutin and quercetin. In conclusion, GBE50DP improved the social behavior, ability of learning and memory in VCI rats, decreased nerve cell damage and protected nerve cells from apoptosis by reducing oxidative stress and inflammation, thereby improving cognitive dysfunction.

Correspondence to: Professor Wen-Lan Li, School of Pharmacy, Harbin University of Commerce, 138 Tongda Street, Daoli, Harbin, Heilongjiang 150076, P.R. China
E-mail: lwldzd@163.com

Professor Hong Li, Research Institute, Zhejiang Shangyao Jiuxu Pharmaceutical Co., Ltd., 398 Xianhua North Street, Wucheng, Jinhua, Zhejiang 321016, P.R. China
E-mail: lh999jd@vip.163.com

Key words: Ginkgo biloba extract, vascular cognitive impairment, social behavior, oxidative stress, inflammatory cytokines, apoptosis, blood-absorbed components

Introduction

Vascular cognitive impairment (VCI) is a symptom of cognitive impairment caused by a variety of cerebrovascular diseases (such as cerebral infarction, cerebral hemorrhage) or vascular risk factors (such as age, heredity, hypertension, hyperlipidemia, diabetes, smoking, alcoholism, obesity and lack of exercise) (1). It can occur alone or is often in conjunction with neurodegenerative diseases, such as Alzheimer's disease (2). Its etiology is complex and diverse and includes brain neurodegenerative diseases, cerebral ischemic and hemorrhagic lesions (3,4), mainly manifested as memory decline, thinking and language disorders and negative emotions (encompassing anxiety, irritability, apathy and depressive mood) (5). The pathogenesis of VCI is ladder-like and may eventually develop into dementia without timely intervention and which, once formed, will be difficult to cure (6,7). The incidence of VCI is increasing year by year (8,9), resulting in a heavy burden on the family and society, which has attracted increasing attention.

Ginkgo biloba extract 50 (GBE50) is an extract of *Ginkgo biloba* leaf that is homologous to both food and medicine, in which the mass fraction of ginkgolic acid is <5 mg/kg, that of flavonol glycosides is >24%, that of terpene lactones is >10% and that of flavonoids is >44% (10,11). The *Ginkgo biloba* preparation has been proved to have a positive effect on relieving ischemic stroke (12) and improves VCI, but its mechanism of action is not completely clear yet. Compared with the traditional *Ginkgo biloba* leaf extract (13), GBE50 has more effective ingredients, rapider effect, fewer potential allergenic components and higher safety (14). The GBE50 dropping

pill (GBE50DP) has the therapeutic effect of activating blood circulation, removing blood stasis and clearing collaterals (15). In the present study, the intervention experiment of GBE50DP on VCI rats was conducted to further understand the efficacy and mechanism of GBE50DP in improving VCI.

Materials and methods

Reagents. GBE50DP was provided by Zhejiang Shangyao Jiuxu Pharmaceutical Co., Ltd. Donepezil hydrochloride tablets were provided by Chongqing Zein Biotechnology Co., Ltd. Pentobarbital sodium was purchased from Merck KGaA. Superoxide dismutase (SOD), malondialdehyde (MDA), glutathione peroxidase (GSH-Px), catalase (CAT), IL-1β, IL-6 and TNF-α kits were provided by Jiangsu Jingmei Biotechnology Co., Ltd. Terminal-deoxynucleotidyl transferase mediated nick end labeling (TUNEL) kit was provided by Roche Diagnostics GmbH. Rabbit two-step immunohistochemical kit (PV-6001) and 3,3'-diaminobenzidine (DAB) were provided by Beijing Zhongshan Jinqiao Biotechnology Co., Ltd. Caspase-3, Bcl-2, Bax, cytochrome *c* (Cyto-C), PARP-1, β-actin monoclonal antibody, HRP-labeled anti-rat and HRP-labeled anti-rabbit secondary antibody were provided by Beijing Bioss Biotechnology Co., Ltd. Fas monoclonal antibody was provided by Thermo Fisher Scientific, Inc. PVDF membrane was acquired from Beijing Biotopped Technology Co., Ltd. Enhanced chemiluminescence (ECL) reagent was purchased from Dalian Meilun Biotechnology Co., Ltd. Tissue lysate and SDS-PAGE kits were provided by Beyotime Biotechnology. A Bradford protein quantification kit was provided by Beijing Lanjieke Technology Co., Ltd. MS-grade formic acid and acetonitrile were acquired from Thermo Fisher Scientific, Inc. All other chemical reagents used were of analytical grade.

Devices. Open field box (100x100x40 cm), Morris water maze (diameter 150 cm, height 50 cm) and eight-arm maze (radial arm 29x6x15 cm) were provided by Anhui Zhenghua Biologic Apparatus Facilities Co., Ltd. Centrifuges (5810R and 5424R) were acquired from Eppendorf SE, a microplate reader (RT-6000) from Rayto Life and Analytical Sciences Co., Ltd., a homogenizer (FA25) from Fluko Shanghai Equipment Co., Ltd., an embedding machine (BM-VII) from Xiaogan Hongye Medical Instrument Co., Ltd., a microtome (CM3050s) from Leica Microsystems GmbH, an optical microscope (BX-53) from Olympus Corporation, a fluorescence microscope (DM4000B) from Leica Microsystems GmbH and a gel imaging system (C300) from Azure Biosystems.

VCI rat model establishment and drug administration. A total of 120 male Wistar rats (weighing 300-340 g; 9-11 weeks) were supplied by the Changchun Yisi Experimental Animal Technology Co., Ltd. [license no., SCXK(Ji)-2023-0002], housed in a temperature- and humidity-controlled environment (25˚C and 60%) and given free access to water and a standard diet.

After 1 week of adaptation, the rats were randomly divided into the control, model, positive (donepezil 0.45 mg/kg) and GBE50DP low-, medium- and high-dose groups (50, 100 and 200 mg/kg, respectively), with 20 rats in each group. Anesthesia was administered by intraperitoneal injection of 40 mg/kg sodium pentobarbital. An incision was then made at the midline position in the neck, and the bilateral common carotid arteries were isolated and exposed. The control group was exposed without ligation, while the other groups were permanently ligated (16,17) and sutured. The drugs were prepared into suspension with 0.5% sodium carboxymethyl cellulose aqueous solution for intragastric administration once a day for 8 weeks, while the control and model group were given the same volume of pure water.

Social behavior test. The experiment was carried out in a dark and quiet environment within the open field box. The rats were placed individually in the box for 5 min twice a day for 2 days, for the adaptive training. At 1 h before the experiment, the tested rat was isolated in a single cage to stimulate its social behavior. The test was performed for 5 min, and the number and duration of contacts were recorded.

Morris water maze test (18). The inner wall of the Morris water maze was made black, and four quadrants were distinguished by different markers. A platform was placed in the center of one of the quadrants, 2 cm below the water level, and the water temperature was controlled at 23.0±2.0˚C. Adaptive training: 1 Day before the experiment, the rats were adapted to the environment in a non-platform pool and swam freely for 1.5 min. Positioning navigation experiment: The rats facing the pool wall were randomly placed in one of the three quadrants without the platform. The time frame from their entering the water to boarding the platform (the escape latency) was recorded. The time frame was recorded as 1.5 min if the platform was not found within 1.5 min, and the rats were then guided to the platform and stayed for 10 sec so that they could perform spatial learning and memory according to the markers. The experiments were performed twice a day, in intervals of 4 h, for 5 days total. The 6th day was set as the test period. Space exploration experiment: The platform was removed on the 6th day, and the residence time of the rats in the target quadrant and the number of times they crossed the original platform location within 1.5 min were recorded.

Eight-arm maze test. The experiment was carried out in a quiet and odorless environment. There was a removable door at the entrance of each arm, and the arms 1, 2, 6 and 7 were set as the food arms. There were 4 adaption tests before the test, 10 min for each per day. On the first day, the bait was placed in the central area; on the second day, it was placed in the central area and the entrance of each arm; on the third day, it was placed on the top of each arm; from the first day to the third day, three rats were placed in the maze at the same time for exploration; on the fourth day, the bait was placed only at the top of the food arm, was placed in the maze individually for exploration. The rats were then trained for 5 days and fasted for 24 h before the training, with no restriction on drinking water. During the training, only bait was placed in the food arms. After the rats were placed in the central area for 15 sec, the doors of each arm were opened, and the foraging of all arms was free for 10 min or completed in advance. Restricted feed was given after each adaptation and training. The times that the rats repeatedly entered the food arm that had been

visited (the working memory errors) and the times that the rats entered the food-free arm (the reference memory errors) were recorded.

Sample collection and processing. After the rats were anesthetized with 3% sodium pentobarbital (40 mg/kg, i.p.), they were fixed in the supine position, and the chest cavity was quickly opened to expose the heart. The perfusion needle was inserted into the aorta through the apex of the left ventricle, and the right atrial appendage was cut open simultaneously. First, 4˚C pre-cooled normal saline (~150 ml) was rapidly perfused until the effluent was clear and the liver turned white; then, 4˚C pre-cooled 4% paraformaldehyde (~200 ml) was perfused for fixation. When the muscles of the rat's limbs and tail became stiff, the rats were immediately decapitated to obtain the brain. The hippocampal tissues were quickly separated on ice and placed in 4% paraformaldehyde for fixation (the volume ratio of fixative solution to tissue was >10:1), fixed at 4˚C for >24 h for subsequent experiments.

After the rats were anesthetized with 3% sodium pentobarbital (40 mg/kg, i.p.), ~1.0 ml of blood was collected from the orbital venous plexus and placed in a heparin sodium anticoagulant tube. After confirming that the rats were in a deep state of anesthesia (with disappearance of the toe clonus reflex), the rats were immediately decapitated to obtain the brain, which was quickly separated into hippocampal tissue on ice, placed in a pre-frozen storage tube, rapidly frozen in liquid nitrogen, and then transferred to -80˚C for storage. The blood samples were centrifuged at 13,523 x g for 10 min at 4˚C to separate the supernatant, which was obtained as the drug-containing plasma. The plasma was frozen at -80˚C for storage. The animal experiment in this study was approved by the Harbin University of Commerce Ethics Committees (approval no. HSDYXY-2023035).

ELISA. The white transparent 'herringbone' hippocampus was collected from the rat brain and quickly transferred to the ice. The tissue was homogenized with pre-cooled PBS at a low temperature until it was completely broken. Following centrifugation at 4˚C, 1,157 x g for 20 min, the supernatant was collected. The contents of SOD (cat. no. JM-01793R1), MDA (cat. no. JM-10323R1), GSH-Px (cat. no. JM-02173R1), CAT (cat. no. JM-10334R1), IL-1β (cat. no. JM-01454R1), IL-6 (cat. no. JM-01597R1) and TNF-α (cat. no. JM-01587R1) were detected by ELISA kits (Jiangsu Jingmei Biotechnology Co., Ltd.) using the microplate reader.

Histopathological observation

Hematoxylin and eosin (H&E) assay. The tissues were fixed using 4% paraformaldehyde (4˚C for >24 h), dehydrated through a graded ethanol series (60% for 4 h, 80% for 4 h, 90% for 4 h, 95% for 4 h twice and 100% for 2 h twice), cleared in xylene (5 min twice), embedded in paraffin (soft wax at 52-54˚C for 30 min, twice; hard wax at 54-56˚C for 30 min, twice), sectioned at a thickness of 4.5 μm, dewaxed by xylene and stained by H&E (19), dehydrated by gradient ethanol and sealed. The damage of nerve tissue in the CA1 region of the hippocampus was observed by optical microscopy (BX-53; Olympus Corporation). For each sample, three random fields of view were captured from this region.

TUNEL assay. Following the TUNEL kit instructions (20), the slices were dewaxed with xylene and rehydrated through a graded ethanol series. The working solution of protease K was added and incubated at 37˚C for 20 min. The slices were rinsed with PBS, TUNEL reaction solution was added and it was incubated in the dark for 60 min at 37˚C. The sections were rinsed with PBS and sealed with an anti-fluorescence quencher. Apoptosis was observed and calculated using a fluorescence microscope (DM4000B; Leica Microsystems GmbH). The apoptosis rate was calculated as: (number of TUNEL-positive cells/total number of cells) x100.

Immunohistochemical method (21). The tissues were fixed with 4% paraformaldehyde, dehydrated, embedded in paraffin and then sectioned (4-μm thickness), repaired with antigen (0.01 M citrate buffer, pH 6.0, boiling water bath for 15 min). Endogenous peroxidase was eliminated with 3% H_2O_2 (reagent 1 of PV-6001 kit; Zhongshan Jinqiao Biotechnology) at room temperature for 10 min, followed by three washes with PBS (3 min each). Sections were incubated with the primary antibody (Caspase-3, bsm-61071R, dilution 1:200; Bcl-2, bs-0032R, dilution 1:200; Bax, bsm-52316R, dilution 1:200; Cyto-C, bsm-52050R, dilution 1:200; PARP-1, bsm-52408R, dilution 1:200; β-actin, bsm-63325R, dilution 1:1,000; Bioss Biotechnology; Fas, MA5-35308, dilution 1:200; Thermo Fisher Scientific, Inc.) overnight at 4˚C, and then incubated with the secondary antibody (HRP-conjugated goat anti-rabbit IgG; reagent 2 of PV-6001 kit) at 37˚C for 20 min. The slices were stained with DAB (Zhongshan Jinqiao Biotechnology) for 5 min at room temperature, counterstained with hematoxylin (room temperature, 20 sec), differentiated with hydrochloric acid alcohol, dehydrated with gradient ethanol, returned to blue with tap water and sealed with neutral gum. Images were captured using an optical microscopy (BX-53; Olympus Corporation). The visual field was randomly selected, and the average optical density in each visual field was measured using ImageJ software (version 1.53a; National Institutes of Health).

Western blotting (22). Hippocampal tissue was collected, cut and ground in liquid nitrogen. Lysis solution (RIPA lysis buffer; Beyotime Biotechnology) was added to the tissue overnight at 4˚C. Following centrifugation at 4˚C, 13,523 x g for 10 min, the supernatant was collected and stored at -80˚C. The protein content was determined and quantified (Bradford protein quantification kit, Lanjieke Technology). The sample was mixed with the loading buffer and denatured at 95˚C for 10 min (30 μg/lane). Gel electrophoresis was performed (SDS-PAGE kit; Beyotime Biotechnology) at a voltage of 50 V. The protein bands were transferred to the PVDF membrane, sealed with 5% skimmed milk powder for 1 h (room temperature), then incubated with a primary antibody (Caspase-3, bsm-61071R, dilution 1:1,000; Bcl-2, bs-0032R, dilution 1:1,000; Bax, bsm-52316R, dilution 1:1,000; Cyto-C, bsm-33193M, dilution 1:2,000; PARP-1, bsm-52408R, dilution 1:500; β-actin, bsm-63325R, dilution 1:50,000; Bioss Biotechnology; Fas, MA5-35308, dilution 1:1,000; Thermo Fisher Scientific, Inc.) at 4˚C overnight, and incubated with HRP-labeled secondary antibody (HRP-conjugated goat anti-rat, bs-0293G-HRP, dilution 1:5,000; HRP-conjugated goat anti-rabbit, bs-0295G-HRP, dilution 1:5,000; Bioss Biotechnology) at 37˚C for 1 h. The

membranes were exposed with ECL (ECL reagent; Meilun Biotechnology) and then images captured and analyzed using a gel imaging system (C300; Azure Biosystems).

Liquid chromatography-tandem mass spectrometry (LC-MS/MS) assay. After 8 weeks of intragastric administration of GBE50DP, the orbital blood was collected, and the samples were processed. A total of 200 μl plasma was taken, and 400 μl pre-cooled acetonitrile was added, vortexed and mixed for 5 min, centrifuged at 9,391 x g for 10 min at 4˚C, and the supernatant was filtered using a 0.45 μm microporous membrane for injection analysis. The chemical components of GBE50DP were analyzed respectively in positive and negative ion modes by LC-MS/MS technology, and the chemical components of blank plasma and drug-containing plasma were compared.

The high-performance liquid chromatography (HPLC) analysis was conducted on an e2695 system (Waters Corporation) with an HSS T3 column (2.1x100 mm, 1.7 μm, Waters Corporation). The mobile phase consisted of 0.1% formic acid-water and 0.1% formic acid-acetonitrile with a flow rate of 0.3 ml/min according to the gradient elution program: 5-20% B (0-3 min), 20-100% B (3-15 min). The temperature of the column was 30˚C. The injection volume was set at 5 μl.

Mass spectrometry (MS) detection was performed on a Triple TOF 5600 system (Shanghai AB SCIEX Analytical Instrument Trading Co.) equipped with an electrospray ionization. MS data acquisition was achieved by the positive and negative ion modes, and the ion source voltages were 5.5 and -4.5 kV, respectively. The ion source temperature was 550˚C. The declustering potential was 40/-40 V, and the collision energy to 20/-20 V. Nitrogen was used as an atomizer and auxiliary gas. The sprayer gas (Gas 1) and heater gas (Gas 2) were both 55 psi, and the curtain gas was 35 psi. Information-dependent acquisition set eight peaks with response values exceeding 100 cps for secondary mass spectrometry scanning. Time-of-flight MS and tandem MS (MS/MS) were scanned within the mass range of m/z 80-1,600 Da.

Statistical analysis. SPSS 22.0 statistical software (IBM Corp.) was used for statistical analysis. Data are expressed as the mean ± standard deviation. One-way analysis of variance followed by Tukey's post hoc test was used for difference analysis between groups if the data conformed to normal distribution. The rank sum test was used for difference analysis between groups if the data did not conform to normal distribution. P<0.05 was considered to indicate statistical significance. Graphs were prepared using GraphPad Prism 6.0 software (Dotmatics).

Results

Results of social behavior test. As shown in Table I, the number of contacts in the model group rats was (8±8) times and the contact duration was 67.21±45.61 sec, both significantly lower than those in the control group (16±4 times, 151.57±30.59 sec; P<0.001). Compared with the model group, the number of contacts (12±6) times and contact duration (111.61±48.75) sec in the GBE50DP high-dose group rats were significantly increased (P<0.05).

Table I. Effects of GBE50DP on the number and duration of contacts (n=12).

Group	Number of contacts	Duration of contacts (sec)
Control	16±4	151.57±30.59
Model	8±8[a]	67.21±45.61[a]
Donepezil	13±6[b]	130.42±49.31[b]
GBE50DP-L	12±2[c]	106.50±45.34[c]
GBE50DP-M	12±5[c]	96.26±32.84
GBE50DP-H	12±6[c]	111.61±48.75[c]

[a]P<0.001 vs. Control group; [b]P<0.01 and [c]P<0.05 vs. Model group. GBE50DP, *Ginkgo biloba* extract 50 dropping pill; -L, low dose group; -M, medium dose group; -H, high dose group.

Table II. Effect of GBE50DP on the number of crossing platforms (n=12).

Group	Number of platforms crossings
Control	2.6±1.6
Model	1.4±1.0[a]
Donepezil	2.8±1.3[b]
GBE50DP-L	2.4±1.4
GBE50DP-M	2.6±1.2[b]
GBE50DP-H	2.9±1.3[c]

[a]P<0.05 vs. Control group; [b]P<0.05 and [c]P<0.01 vs. Model group. GBE50DP, *Ginkgo biloba* extract 50 dropping pill; -L, low dose group; -M, medium dose group; -H, high dose group.

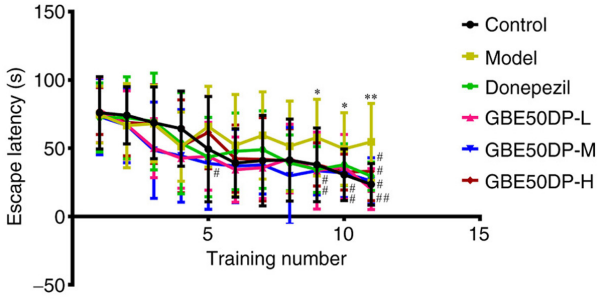

Figure 1. Effect of GBE50DP on escape latency (n=12). *P<0.05 and **P<0.01 vs. Control group; #P<0.05 and ##P<0.01 vs. Model group. GBE50DP, *Ginkgo biloba* extract 50 dropping pill; -L, low dose group; -M, medium dose group; -H, high dose group.

Results of Morris water maze test. The results of the positioning navigation experiment are shown in Fig. 1. Compared with the control group, the escape latency of rats in the model group was significantly prolonged at the 9, 10 and 11th trials (P<0.05 or P<0.01). Compared with the model group, the escape latency of rats in the donepezil group was significantly shortened at the 11th trial (P<0.05), that of rats in the

Table III. Effect of GBE50DP on the indexes of the eight-arm maze (n=12).

Group	Number of working memory errors	Number of reference memory errors	Foraging completion time (min)
Control	1.9±0.8	2.5±1.3	5.04±2.28
Model	3.4±1.1[a]	4.8±1.2[a]	7.24±0.61[b]
Donepezil	1.8±1.0[c]	2.8±1.0[c]	4.83±0.80[c]
GBE50DP-L	2.0±0.8[c]	3.6±1.5	5.27±1.59[c]
GBE50DP-M	2.0±0.7[c]	3.0±0.7[c]	5.64±0.58
GBE50DP-H	2.3±1.0	2.8±0.5[c]	4.64±1.22[d]

[a]P<0.05 and [b]P<0.01 vs. Control group; [c]P<0.05 and [d]P<0.01 vs. Model group. GBE50DP, *Ginkgo biloba* extract 50 dropping pill; -L, low dose group; -M, medium dose group; -H, high dose group.

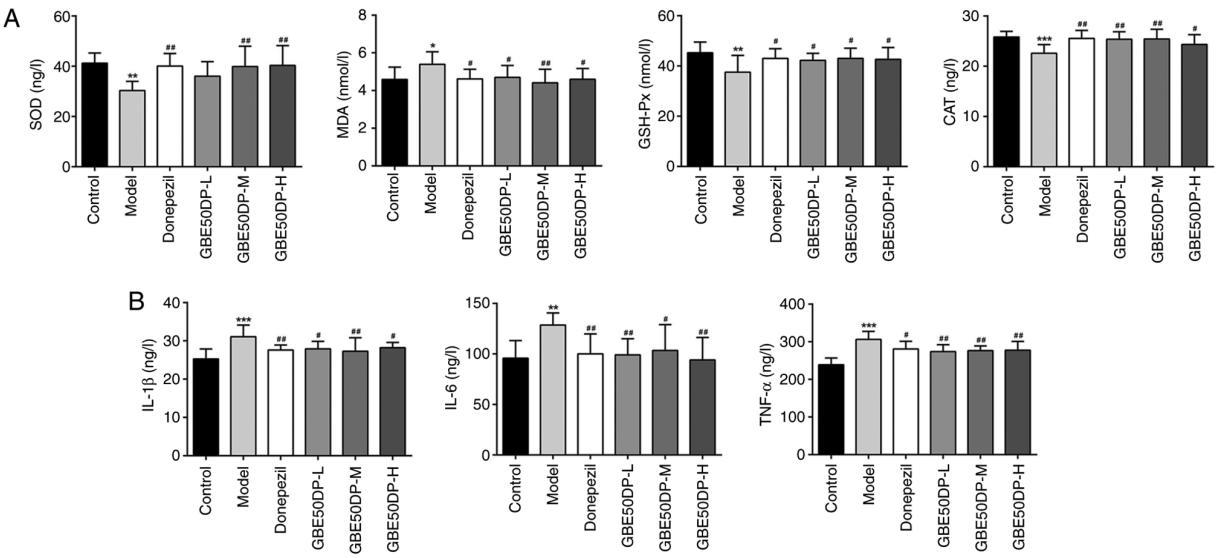

Figure 2. Effects of GBE50DP on oxidative stress and inflammation in the hippocampus. (A) Effect of GBE50DP on the contents of SOD, MDA, GSH Px and CAT in the hippocampus (n=8); (B) Effect of GBE50DP on the contents of IL-1β, IL-6 and TNF-α in the hippocampus (n=8). [*]P<0.05, [**]P<0.01 and [***]P<0.001 vs. Control group; [#]P<0.05 and [##]P<0.01 vs. Model group. GBE50DP, *Ginkgo biloba* extract 50 dropping pill; SOD, superoxide dismutase; MDA, malondialdehyde; GSH Px, glutathione peroxidase; CAT, catalase; -L, low dose group; -M, medium dose group; -H, high dose group.

GBE50DP-L group was significantly shortened at the 9 and 11th trials (P<0.05 or P<0.01), that of rats in the GBE50DP-M group was significantly shortened at the 5, 9, 10 and 11th trials (P<0.05), and that of rats in the GBE50DP-H group was significantly shortened at the 10 and 11th trials (P<0.05).

The results of space exploration experiments are shown in Table II. Compared with the control group, the number of platform crossings of rats in the model group was significantly decreased (P<0.05). Compared with the model group, the number of platform crossings in the positive, GBE50DP-M and GBE50DP-H groups was significantly increased (P<0.05 or P<0.01).

Results of eight-arm maze test. As shown in Table III, compared with the control group, the average number of working memory errors and reference memory errors of rats in the model group was significantly increased (P<0.05), and the foraging completion time was significantly prolonged (P<0.01). Compared with the model group, the mean number of working memory errors of rats in the positive, GBE50DP-L and -M groups was significantly decreased (P<0.05), that of reference memory errors of rats in the positive, GBE50DP-M and -H groups was significantly decreased (P<0.05), and the foraging completion time of the positive, GBE50DP-L and -H groups was significantly decreased (P<0.05 or P<0.01).

Results of oxidative stress and inflammatory marker detection in the rat hippocampus

Content of oxidative stress indicators. As shown in Fig. 2A, compared with the control group, the SOD content in the hippocampal tissue of the model group rats (30.31±3.67 ng/l) was significantly decreased (P<0.01), the GSH-Px content (37.51±6.70 nmol/l) was significantly decreased (P<0.01), the CAT content (22.59±1.72 ng/l) was significantly decreased (P<0.001), while the MDA content (5.39±0.67 nmol/l) was significantly increased (P<0.05). Compared with the model group, the SOD content (40.32±7.88 ng/l) in the GBE50DP high-dose group was significantly increased (P<0.01), the GSH-Px content (42.62±4.77 nmol/l) was significantly

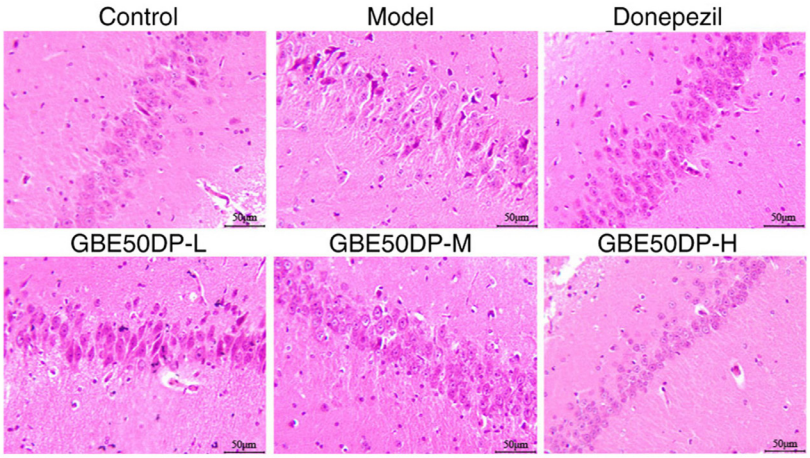

Figure 3. H&E staining results of the hippocampal CA1 region (scale bar, 50 μm). H&E, hematoxylin & eosin. GBE50DP, *Ginkgo biloba* extract 50 dropping pill; -L, low dose group; -M, medium dose group; -H, high dose group.

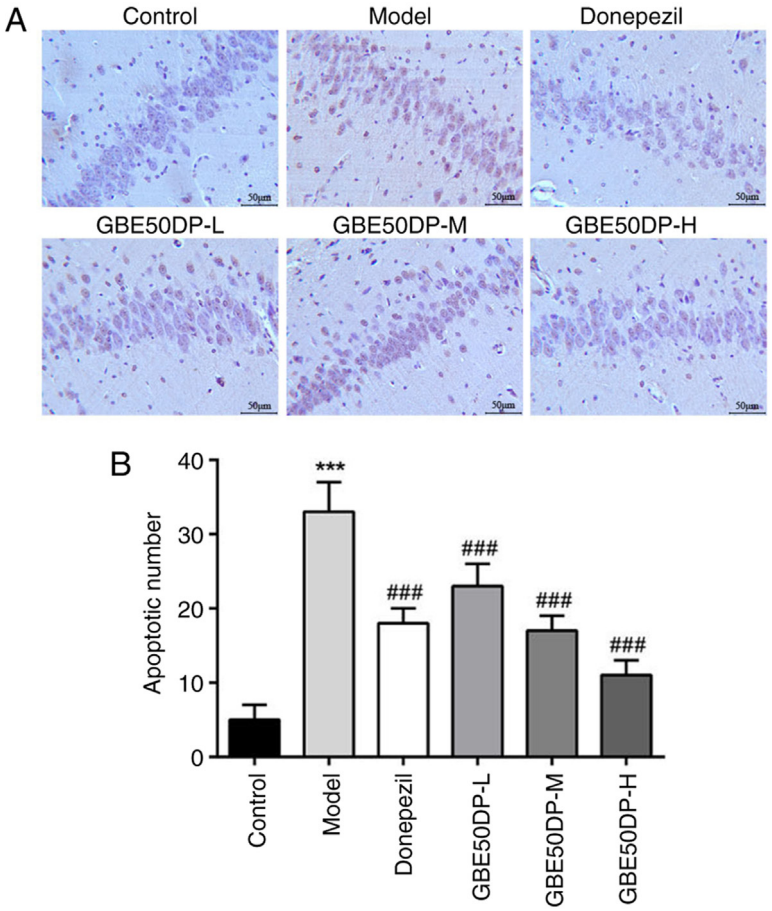

Figure 4. Effect of GBE50DP on neuronal apoptosis in the hippocampal CA1 region. (A) TUNEL staining results of the hippocampal CA1 region (scale bar 50 μm). (B) Number of apoptotic cells in the hippocampal CA1 region (n=3). ***P<0.001 vs. Control group; $^{###}$P<0.001 vs. Model group. GBE50DP, *Ginkgo biloba* extract 50 dropping pill; -L, low dose group; -M, medium dose group; -H, high dose group.

increased (P<0.05), the CAT content (24.33±1.96 ng/l) was significantly increased (P<0.05), while the MDA content (4.60±0.57 nmol/l) was significantly decreased (P<0.05).

Content of inflammatory indicators. As shown in Fig. 2B, compared with the control group, the IL-1β content (31.08±3.03 ng/l) in the hippocampal tissue of the model group rats was significantly increased (P<0.001), the IL-6 content (128.50±12.07 ng/l) was significantly increased (P<0.01), and the TNF-α content (306.16±21.47 ng/l) was significantly increased (P<0.001). Compared with the model group, the IL-1β content (28.21±1.37 ng/l) in the GBE50DP high-dose group was significantly decreased (P<0.05), the IL-6 content (94.03±22.27 ng/l) was significantly decreased (P<0.01) and

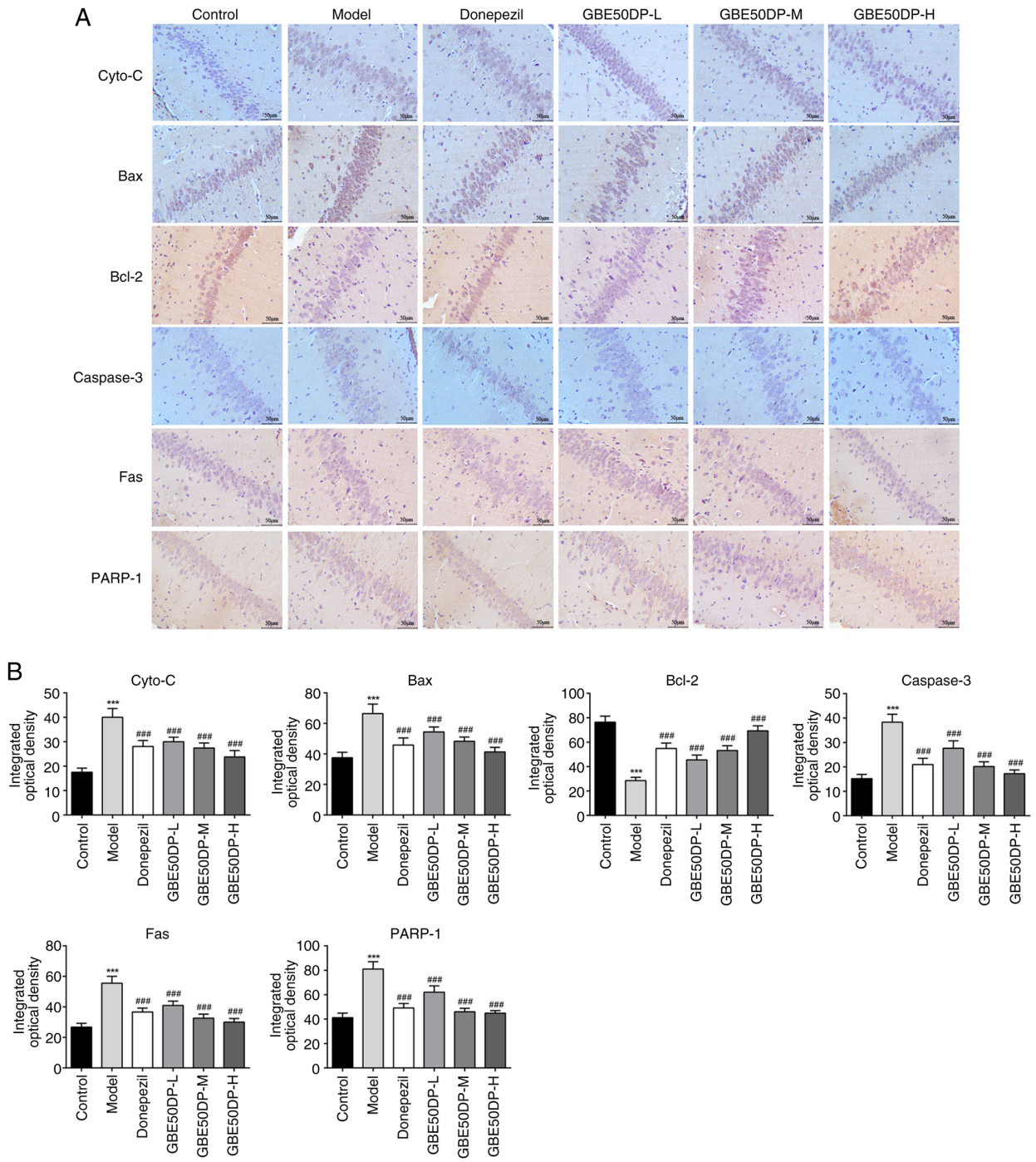

Figure 5. Effect of GBE50DP on the expression of apoptosis-related proteins in the hippocampal CA1 region. (A) Expression of Cyto-C, Bax, Bcl-2, Caspase-3, Fas and PARP-1 in the hippocampal CA1 region (scale bar, 50, μm). (B) Integral optical densities of Cyto-C, Bax, Bcl-2, Caspase-3, Fas, and PARP-1 in the hippocampal CA1 region (n=3). ***P<0.001 vs. Control group; $^{###}$P<0.001 vs. Model group. Cyto-C, cytochrome *c*; PARP-1 Poly (ADP-ribose) polymerase 1; GBE50DP, *Ginkgo biloba* extract 50 dropping pill; -L, low dose group; -M, medium dose group; -H, high dose group.

the TNF-α content (277.42±23.28 ng/l) was significantly decreased (P<0.01).

Morphological changes of neurons in the CA1 region of the rat hippocampus

Results of H&E assay. As shown in Fig. 3, in the control group, the nerve cells were arranged neatly, the cytoplasm and nucleus were stained clearly, and no inflammatory cell infiltration, capillary dilation or congestion was observed. Compared with the control group, the structure of the hippocampal CA1 region of rats in the model group was loose, the arrangement of nerve cells was irregular and the morphology was incomplete, the cytoplasm was deeply stained, the nuclear condensation, apoptotic bodies and glial cells were improved increased, the inflammatory cells were scattered, and the capillaries were dilated. Compared with the model group, the aforementioned pathological changes in each administration group were improved to various degrees, showing a tighter structure, a decrease in the number of apoptotic bodies and glial cells, and an improvement in telangiectasia. Among them, the

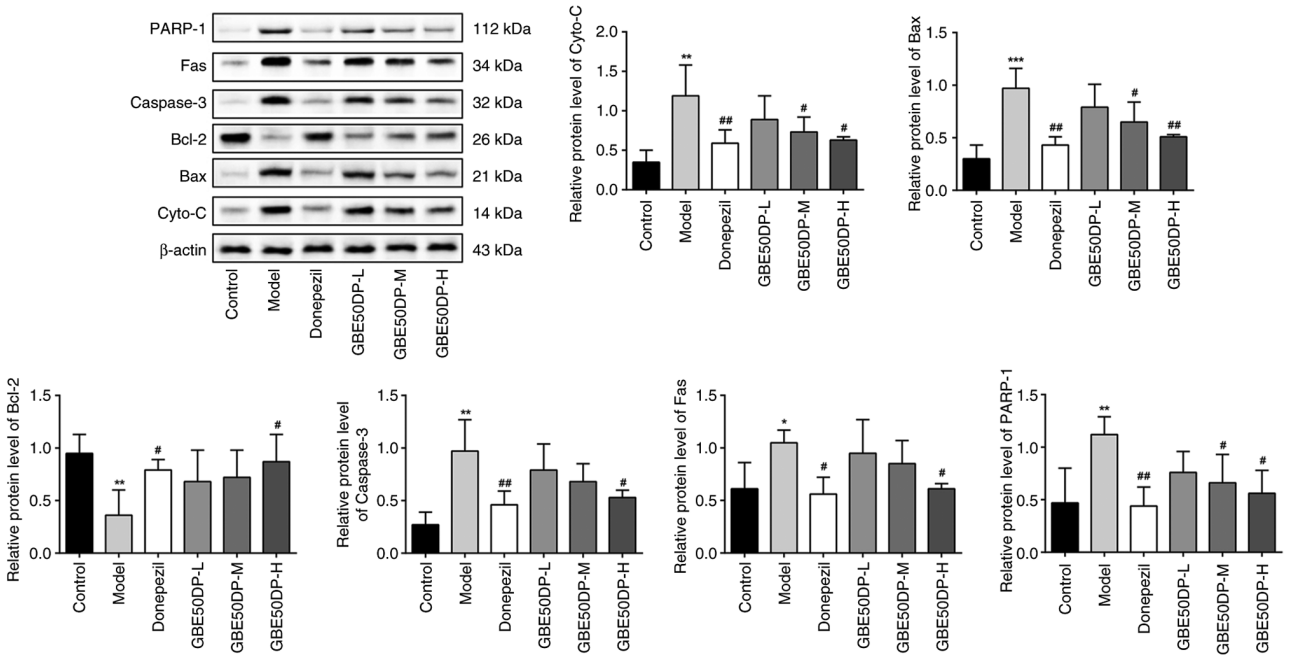

Figure 6. Relative expression levels of Cyto-C, Bax, Bcl-2, Caspase-3, Fas and PARP-1 in the hippocampal CA1 region. Western blot bands and quantified bar charts of each protein, n=3. *P<0.05, **P<0.01 and ***P<0.001 vs. Control group; $^{\#}$P<0.05 and $^{\#\#}$P<0.01 vs. Model group. Cyto-C, cytochrome *c*; PARP-1 Poly (ADP-ribose) polymerase 1; GBE50DP, *Ginkgo biloba* extract 50 dropping pill; -L, low dose group; -M, medium dose group; -H, high dose group.

improvement in the GBE50DP-H group was the most obvious, followed by the positive group.

Results of the TUNEL assay. As shown in Fig. 4, the number of apoptotic neurons in the CA1 region of the hippocampus in the control group rats was 5±2, while in the model group it was 33±4. Compared with the control group, the number of apoptotic neurons in the model group was significantly increased (P<0.001). Compared with the model group, the number of apoptotic neurons in all treatment groups was significantly decreased (P<0.001), with the GBE50DP high-dose group showing the most pronounced change, having 11±2 apoptotic neurons.

Results of the immunohistochemical assay. As shown in Fig. 5, compared with the control group, the expression of Bcl-2 in the hippocampal CA1 region of rats in the model group was significantly decreased (P<0.001), while that of Cyto-C, Bax, Caspase-3, Fas and PARP-1 was significantly increased (P<0.001). Compared with the model group, the expression of Bcl-2 in the hippocampal CA1 region of rats in each administration group was significantly increased (P<0.001), while that of Cyto-C, Bax, Caspase-3, Fas and PARP-1 was significantly decreased (P<0.001), particularly in the GBE50DP-H group.

Results of western blot analysis. As shown in Fig. 6, compared with the control group, the expression of Bcl-2 in the hippocampal CA1 region of rats in the model group was significantly decreased (P<0.05), while the expression of Cyto-C, Bax, Caspase-3, Fas and PARP-1 were significantly increased (P<0.05 or P<0.01 or P<0.001). Compared with the model group, the expression of Bcl-2 in the hippocampal CA1 region of rats in the positive group and the GBE50DP-H group significantly was increased (P<0.05), while that of Cyto-C, Bax, Caspase-3, Fas and PARP-1 in the positive and GBE50DP-H groups was significantly decreased (P<0.05 or P<0.01).

Analysis of components of GBE50DP-containing plasma. The molecular formula of the compound in the GBE50DP-containing plasma was speculated by ion peak and cleavage law (see Fig. 7). The main VCI-related compounds were speculated as the ginkgolide A, B, C, K, bilobalide, rutin and quercetin.

Discussion

One of the clinical characteristics of VCI is social disorder (23), which is manifested by social withdrawal, decreased active communication, weakened empathy and language communication disorders. The experimental results of the present study showed that GBE50DP (especially at high dose) can significantly shorten the escape latency of VCI rats, increase the number of platform crossings, and reduce errors in working memory and reference memory. This suggested that it can effectively improve learning and memory abilities, providing an experimental basis for clinical application to improve the cognitive and social functions of VCI patients. In addition, GBE50DP can significantly increase the activities of SOD and GSH-Px in the hippocampus, reduce the levels of IL-1β and TNF-α, increase the expression of Bcl-2 and decrease that of Bax and Caspase-3. This indicated that it exerts anti-VCI effects through multiple aspects, such as regulating oxidative stress, neuroinflammation and apoptosis pathways, providing ideas for the development of multi-target therapeutic drugs. At the same time, GBE50DP can alleviate neuronal damage and apoptosis in the CA1 region of the hippocampus, suggesting that it may be applicable for early intervention in VCI and delaying the progression of the disease. In the present study, intragastric administration was used, which was consistent

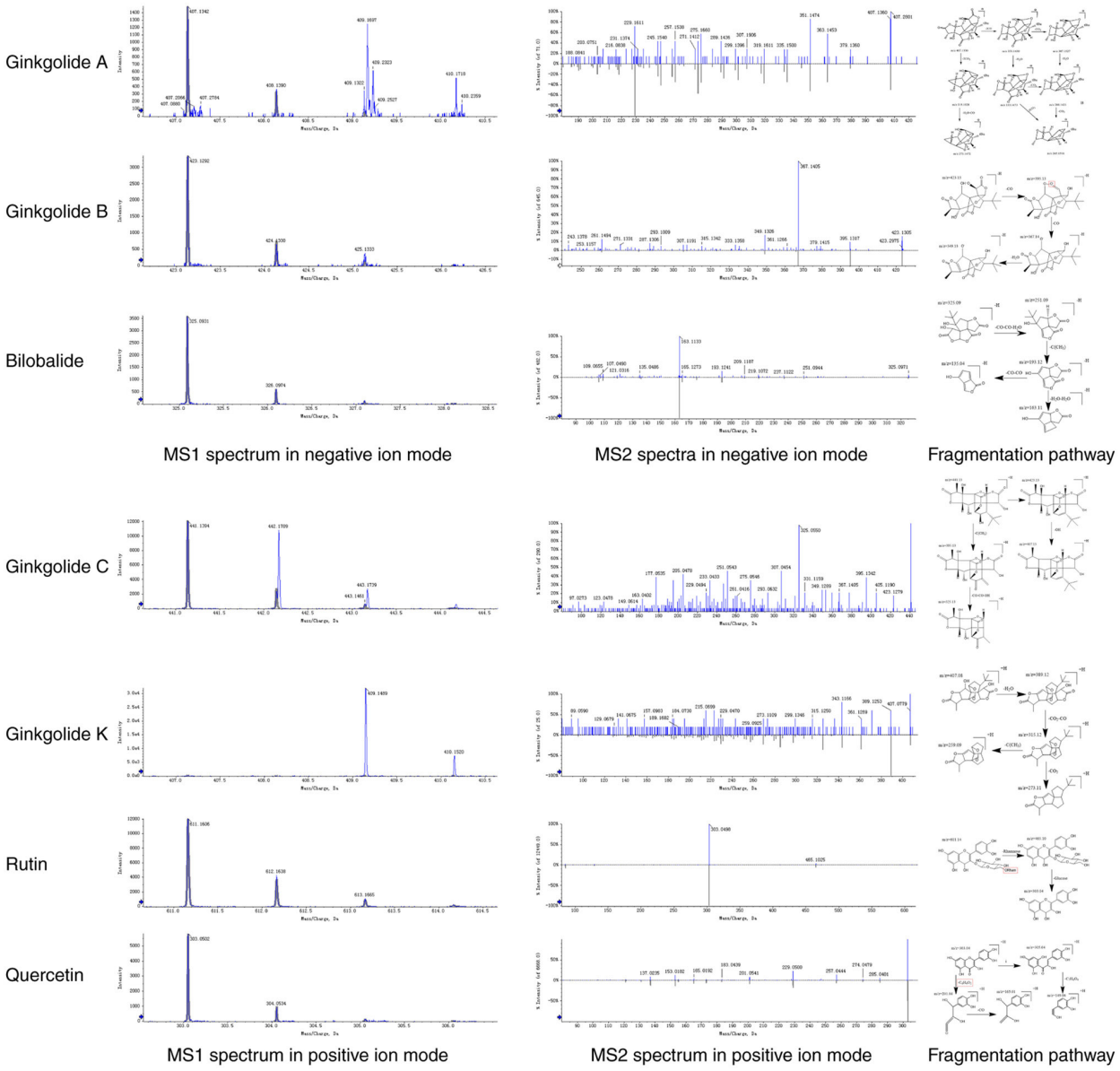

Figure 7. MS1 and MS2 spectra of the compounds in positive and negative ion modes and fragmentation pathway of the compounds.

with the clinical oral preparation route, and the components of GBE50DP in the blood were clear, which showed good potential for clinical transformation.

Ischemic brain injury is one of the strongest stimuli that induces abnormal gene expression, causing mitochondrial dysfunction and cellular apoptosis when the accumulation of reactive oxygen species exceeds the cellular clearance ability (24,25). The results of the *in vivo* experiments demonstrated that, in the VCI model, the activity of the crucial anti-oxidative enzymes (SOD, CAT and GSH-Px) in the hippocampal CA1 region [the key structural region involved in learning and memory (26)], was inhibited due to the increase of oxidative stress caused by vascular lesions, resulting in the increase of MDA [the production of lipid peroxidation (27)] and recruitment of the pro-inflammatory cytokines [IL-1β, IL-6 and TNF-α (28)] through a synergistic effect during ischemic injury (29). The expression changes of the crucial nodes involved in the apoptotic signaling pathway exhibited have proven those oxidative stress-induced apoptotic processes: The Cyto-C released at the initial stage of apoptosis following the vasculopathy in the VCI model, across the rupture of the mitochondrial outer membrane induced by the increase of the pro-apoptotic protein, Bax, and decrease of the anti-apoptotic protein Bcl-2. Caspase-3 was then activated by the death receptor Fas and cleaved multiple cell substrates, leading to apoptosis as the key executor (30). The excessive activation of PARP-1, as an DNA repair enzyme, depleted cellular energy and promoted apoptosis (31,32). The opposite tendency of all the aforementioned indicators following the administration revealed that GBE50DP effectively improved VCI symptoms by enhancing the activity of anti-oxidative enzymes and inhibiting the apoptotic process, thereby protecting cognitive function. This protective effect was reflected in the pathological improvement, as demonstrated by morphological observation using the staining methods.

Previous studies have shown that the *Ginkgo biloba* extract can improve learning and memory abilities by scavenging oxygen free radicals, enhancing antioxidant enzyme activity

and inhibiting neuroinflammation (33), and can safely and effectively improve the mental state and daily living ability of VCI patients (34). In the present study, GBE50DP, as a high-purity *Ginkgo biloba* extract with >50% total flavonoids and terpene lactones, has advantages in neuroprotection (10). GBE50DP can not only inhibit oxidative stress and inflammatory response, but also regulate mitochondrial apoptotic pathways, such as downregulate pro-apoptotic proteins Cyto-C and Bax and upregulate anti-apoptotic protein Bcl-2, thereby reducing hippocampal neuron damage. The high-dose group of GBE50DP was superior to the positive drug donepezil in the number of crossing the platform, the time required to complete foraging and the protection of neurons, which may be associated with the following factors: GBE50DP has a higher concentration of active ingredients and improved bioavailability; the lipid-soluble component ginkgolide B can easily pass through the blood-brain barrier and has a faster onset, and as a natural platelet activating factor (PAF) antagonist, it can improve cerebral microcirculation by inhibiting PAF activity (35); the antioxidant effect of rutin and quercetin form a synergistic effect with the anti-inflammatory effect of ginkgolides, and further regulate the mitochondrial apoptosis pathway. The aforementioned results indicated that GBE50DP has the advantage of improving VCI, suggesting that GBE50DP is expected to be developed as a new preparation for clinical treatment of VCI to expand its indications.

Studies have found that ginkgolide (including ginkgolide A, B, C and K, etc.) and bilobalide belong to the terpene lactones, which can regulate the expression of Bcl-2/Bax to inhibit neuronal apoptosis (36) and play a neuroprotective role in ischemic brain injury (37), thereby improving cognitive ability. Among them, ginkgolide B is the strongest platelet-activating factor antagonist found so far that has a significant antithrombotic effect; ginkgolide A, K and bilobalide can scavenge free radicals (38) and resist cytotoxicity by anti-lipid peroxidation (39); ginkgolide C and bilobalide can inhibit inflammatory responses (40,41). Rutin and quercetin belong to the flavonoid family, which has antioxidant effects such as scavenging free radicals, enhancing SOD activity in brain tissue and reducing MDA content and can improve mitochondrial function, as well as learning and memory ability (42,43). Furthermore, the molecular targets of the effective components would be clarified through molecular interaction and molecular docking. Combined with pharmacokinetic studies, the metabolic parameters of each component *in vivo* and the interactions between components can then be analyzed to clarify their efficacy, thereby verifying the pharmacodynamic material basis and mechanism of GBE50DP.

In the present study, GBE50DP increased the activities of SOD and GSH-Px and decreased the levels of IL-1β and TNF-α, while the aforementioned inflammatory factors were often highly expressed in the cerebrospinal fluid of clinical VCI patients, suggesting that GBE50DP may improve cognitive function through antioxidant and anti-inflammatory dual activities, which provides an experimental basis for its application. It has been reported that GBE50 can exert anti-inflammatory effects by inhibiting the NF-κB signaling pathway (44) and can increase the activities of SOD and GSH-Px (10). Nuclear factor erythroid 2-related factor 2 (Nrf2)/heme oxygenase-1 (HO-1) is a key upstream pathway for regulating these antioxidant enzymes. The results of the present study were highly consistent with the aforementioned mechanism. In addition, PARP-1 can regulate NF-κB activity and promote the expression of inflammatory factors (45). After GBE50DP downregulates PARP-1, the inflammatory factors also decrease. Based on this hypothesis, the protective effect of GBE50DP in VCI may not depend on a single pathway, but may be achieved by activating the Nrf2/HO-1 signaling pathway to combat oxidative stress, inhibiting the NF-κB signaling pathway to alleviate neuroinflammation and synergistically regulating the apoptotic pathway. Subsequent studies can further verify the mechanism of GBE50DP by constructing a cell injury model induced by H_2O_2 or lipopolysaccharides (LPS), combining PARP-1 gene knockout animals or specific inhibitors, and using a composite etiology VCI animal model to provide a more substantial theoretical basis for its clinical transformation.

In conclusion, long-term cerebral hypoperfusion caused by blocking the cervical artery of rats can lead to pathological changes such as hypoxia, neuronal damage, inflammatory response and apoptosis in brain tissue, in turn leading to the symptoms of cognitive impairment. GBE50DP can improve the social behavior and ability of learning and memory, decrease oxidative stress, inhibit inflammatory response, improve the pathological morphology of the hippocampus, protect neurons and protect nerve cells from apoptosis of VCI rats induced by cerebral hypoperfusion, thereby enhancing the self-protection ability of the brain and promoting the improvement of cognitive function. The effective substances of GBE50DP in improving VCI has been preliminarily determined. Those results provided an experimental basis for the further understanding of the neuroprotective effects of GBE50DP and helped reveal the potential of GBE50DP in the treatment of cognitive impairment.

Acknowledgements

Not applicable.

Funding

The present study was supported by the Technical Service Project of Zhejiang Shangyao Jiuxu Pharmaceutical Co., Ltd. (grant no. HT20220012).

Availability of data and materials

The data generated in the present study may be requested from the corresponding author. The data that support the findings of this study have been deposited into CNSA with accession number CNP0009414 (https://doi.org/10.26036/CNP0009414).

Authors' contributions

FLW performed the research and wrote the manuscript. WLL and HL designed the study. FLW, WLL and HL analyzed the data and revised the manuscript. FLW and HL confirm the

authenticity of all the raw data. All authors read and approved the final manuscript.

Ethics approval and consent to participate

The animal experiment in this study was approved by the Harbin University of Commerce Ethics Committees (approval no. HSDYXY-2023035).

Patient consent for publication

Not applicable.

Competing interests

Zhejiang Shangyao Jiuxu Pharmaceutical Co., Ltd., provided the GBE50DP free of charge, and the author HL is affiliated to this company. The authors declare that they have no other competing interests.

References

1. Zanon Zotin MC, Sveikata L, Viswanathan A and Yilmaz P: Cerebral small vessel disease and vascular cognitive impairment: From diagnosis to management. Curr Opin Neurol 34: 246-257, 2021.
2. Cheng YW, Chiu MJ, Chen YF, Cheng TW, Lai YM and Chen TF: The contribution of vascular risk factors in neurodegenerative disorders: From mild cognitive impairment to Alzheimer's disease. Alzheimers Res Ther 12: 91, 2020.
3. Markus HS and Joutel A: The pathogenesis of cerebral small vessel diseases and vascular cognitive impairment. Physiol Rev 105: 1075-1171, 2025.
4. Rajeev V, Chai YL, Poh L, Selvaraji S, Fann DY, Jo DG, De Silva TM, Drummond GR, Sobey CG, Arumugam TV, *et al*: Chronic cerebral hypoperfusion: A critical feature in unravelling the etiology of vascular cognitive impairment. Acta Neuropathol Commun 11: 93, 2023.
5. Jiménez-Ruiz A, Aguilar-Fuentes V, Becerra-Aguiar NN, Roque-Sanchez I and Ruiz-Sandoval JL: Vascular cognitive impairment and dementia: A narrative review. Dement Neuropsychol 18: e20230116, 2024.
6. Rundek T, Tolea M, Ariko T, Fagerli EA and Cemargo CJ: Vascular cognitive impairment (VCI). Neurotherapeutics 19: 68-88, 2022.
7. Chang Wong E and Chang Chui H: Vascular cognitive impairment and dementia. Continuum (Minneap Minn) 28: 750-780, 2022.
8. Pérez Palmer N, Trejo Ortega B and Joshi P: Cognitive impairment in older adults: Epidemiology, diagnosis, and treatment. Psychiatr Clin North Am 45: 639-661, 2022.
9. Kalaria RN, Akinyemi RO, Paddick SM and Ihara M: Current perspectives on prevention of vascular cognitive impairment and promotion of vascular brain health. Expert Rev Neurother 24: 25-44, 2024.
10. Xia CY, Zhou MM, Dong XW, Zhao Y, Jiang MF, Zhu GQ and Zhang ZX: *Ginkgo biloba* extract inhibits hippocampal neuronal injury caused by mitochondrial oxidative stress in a rat model of Alzheimer's disease. PLoS One 19: e0307735, 2024.
11. Tang Z, Jiang DZ, Zhao XX and Zhang YW: Comparison of different specifications of *Ginkgo biloba* extract and discussion on specification improvement. Drug Stand China 21: 21-25, 2020.
12. Liu J, Zhou J, Li WW, Chen YP and Wang J: Effects of different doses of *Ginkgo biloba* extract on cognitive function and neurotransmitter level in rats with vascular cognitive impairment. Chin J Difficult Complicat Cases 20: 182-186, 2021.
13. Liu LM, Wang YT, Zhang JC and Wang SF: Advances in the chemical constituents and chemical analysis of *Ginkgo biloba* leaf, extract, and phytopharmaceuticals. J Pharm Biomed Anal 193: 113704, 2021.
14. Li XY and Liu AJ: Chemical constitution and pharmacological mechanism of *Ginkgo biloba* extract 50 in the treatment of vascular related diseases. Chin Pharm J 59: 1074-1081, 2024.
15. Qian YY, Zhu GQ, Wang WJ and Gao Q: Research progress on the clinical and pharmacological effects of *Ginkgo biloba* extract 50 and its preparations. Chin Tradit Patent Med 43: 998-1003, 2021.
16. Bhat JA and Kumar M: Neuroprotective effects of theobromine in permanent bilateral common carotid artery occlusion rat model of cerebral hypoperfusion. Metab Brain Dis 37: 1787-1801, 2022.
17. Wu S, Huang R, Zhang R, Xiao C, Wang L, Luo M, Song N, Zhang J, Yang F, Liu X and Yang W: Gastrodin and gastrodigenin improve energy metabolism disorders and mitochondrial dysfunction to antagonize vascular dementia. Molecules 28: 2598, 2023.
18. Shrief AI, Elshenawy DS, Elsukary AE, Elekhtiar SA and Yahia OA: Behavioral and histological study on the neuroprotective effect of thymoquinone on the cerebellum in AlCl3-induced neurotoxicity in rats through modulation of oxidative stress, apoptosis, and autophagy. J Mol Histol 56: 81, 2025.
19. Schneider MA, Heeb L, Beffinger MM, Pantelyushin S, Linecker M, Roth L, Lehmann K, Ungethüm U, Kobold S, Graf R, *et al*: Attenuation of peripheral serotonin inhibits tumor growth and enhances immune checkpoint blockade therapy in murine tumor models. Sci Transl Med 13: eabc8188, 2021.
20. Yavari N, Nadia Sharifi Z, Rekabdar Y and Movassaghi S: Protective effect of curcumin on CA1 region of hippocampus in rat model of ischemia/reperfusion injury. Galen Med J 11: e1062, 2022.
21. Yu L, Jin W, Deng D, Wang Y, Chen Q, Zhang Y, Wan H, Chen Y, Chen Y, He Y and Zhang L: Investigation of anti-apoptotic effects and mechanisms of Astragaloside IV in a rat model of cerebral ischemia-reperfusion injury. CNS Neurosci Ther 31: e70209, 2025.
22. Fan LL, Fang H, Zheng JY, Qiu YH, Wu GL, Cai YF, Chen YB and Zhang SJ: Taohong Siwu decoction alleviates cognitive impairment by suppressing endoplasmic reticulum stress and apoptosis signaling pathway in vascular dementia rats. J Ethnopharmacol 333: 118407, 2024.
23. Khan MB, Hoda MN, Vaibhav K, Giri S, Wang P, Waller JL, Ergul A, Dhandapani KM, Fagan SC and Hess DC: Remote ischemic postconditioning: Harnessing endogenous protection in a murine model of vascular cognitive impairment. Transl Stroke Res 6: 69-77, 2015.
24. Li H, Liu Y, Lin LT, Wang XR, Du SQ, Yan CQ, He T, Yang JW and Liu CZ: Acupuncture reversed hippocampal mitochondrial dysfunction in vascular dementia rats. Neurochem Int 92: 35-42, 2016.
25. Ogunro OB, Karigidi ME, Gyebi GA, Turkistani A and Almehmadi AH: Tangeretin offers neuroprotection against colchicine-induced memory impairment in Wistar rats by modulating the antioxidant milieu, inflammatory mediators and oxidative stress in the brain tissue. BMC Complement Med Ther 25: 40, 2025.
26. Rajabian A, Kioumarsi Darbandi Z, Aliyari M, Saberi R, Amirahmadi S, Amini H, Salmani H, Youseflee P and Hosseini M: Pioglitazone improves learning and memory in a rat model of cholinergic dysfunction induced by scopolamine, the roles of oxidative stress and neuroinflammation. Naunyn Schmiedebergs Arch Pharmacol 398: 10221-10237, 2025.
27. Tian Z, Ji X and Liu J: Neuroinflammation in vascular cognitive impairment and dementia: Current evidence, advances, and prospects. Int J Mol Sci 23: 6224, 2022.
28. Yu JY, Fang P, Wang C, Wang XX, Li K, Gong Q, Luo BY and Wang XD: Dorsal CA1 interneurons contribute to acute stress-induced spatial memory deficits. Neuropharmacology 135: 474-486, 2018.
29. Li Y, Ma Y, Dang QY, Fan XR, Han CT, Xu SZ and Li PY: Assessment of mitochondrial dysfunction and implications in cardiovascular disorders. Life Sci 306: 120834, 2022.
30. Guo J, Yang N, Zhang J, Huang Y, Xiang Q, Wen J, Chen Y, Hu T, Liu Q and Rao C: Neurotoxicity study of ethyl acetate extract of Zanthoxylum armatum DC. on SH-SY5Y based on ROS mediated mitochondrial apoptosis pathway. J Ethnopharmacol 319: 117321, 2024.
31. Wang S, Yang Y, Lin J, Zhang W, Yang C, Zhang R, Zhou C, Zhang L, Wang X, Liu J, *et al*: Astragalin actives autophagy and inhibits apoptosis of astrocytes in AD mice via down-regulating Fas/Fasl-VDAC1 pathway. Free Radic Biol Med 232: 72-85, 2025.
32. Jiao Y and Li G: PARP inhibitor PJ34 ameliorates cognitive impairments induced by transient cerebral ischemia/reperfusion through its anti-inflammatory effects in a rat model. Neurosci Lett 764: 136202, 2021.

33. DeFeudis FV and Drieu K: *Ginkgo biloba* extract (EGb761) and CNS functions: Basic studies and clinical applications. Curr Drug Targets 1: 25-58, 2000.
34. Zhan M, Sun L, Liu J, Zeng Z, Shen W, Li H, Wang Y, Han F, Shi J, Zeng X, *et al*: EGb in the treatment for patients with VCI: A systematic review and meta-analysis. Oxid Med Cell Longev 2021: 8787684, 2021.
35. Zhu Q and Liu D: Clinical efficacy and mechanism of *Ginkgo biloba* extract in the treatment of elderly ischemic cerebrovascular disease. Pak J Pharm Sci 37: 705-713, 2024.
36. Hua J, Yin N, Yang B, Zhang J, Ding J, Fan Y and Hu G: Ginkgolide B and bilobalide ameliorate neural cell apoptosis in α-synuclein aggregates. Biomed Pharmacother 96: 792-797, 2017.
37. Feng Z, Sun Q, Chen W, Bai Y, Hu D and Xie X: The neuroprotective mechanisms of ginkgolides and bilobalide in cerebral ischemic injury: A literature review. Mol Med 25: 57, 2019.
38. Ma S, Yin H, Chen L, Liu H, Zhao M and Zhang X: Neuroprotective effect of ginkgolide K against acute ischemic stroke on middle cerebral ischemia occlusion in rats. J Nat Med 66: 25-31, 2012.
39. Zhou LJ, Song W, Zhu XZ, Chen ZL, Yin ML and Cheng XF: Protective effects of bilobalide on amyloid beta-peptide 25-35-induced PC12 cell cytotoxicity. Acta Pharmacol Sin 21: 75-79, 2000.
40. Li B, Zhang B, Li Z, Li S, Li J, Wang A, Hou J, Xu J and Zhang R: Ginkgolide C attenuates cerebral ischemia/reperfusion-induced inflammatory impairments by suppressing CD40/NF-κB pathway. J Ethnopharmacol 312: 116537, 2023.
41. Zhou JM, Gu SS, Wang HM, Zhou J, Wang ZZ and Xiao W: Ginkgolides and bilobalide protect BV2 microglia cells against OGD/reoxygenation injury by inhibiting TLR2/4 signaling pathways. Cell Stress Chaperones 21: 1037-1053, 2016.
42. Mao YJ, Feng YL, Wang MJ, Lyu ZY and Zhai GY: Research progress on rutin derivatives. Zhongguo Zhong Yao Za Zhi 46: 4654-4665, 2021 (In Chinese).
43. Park DJ, Shah FA and Koh PO: Quercetin attenuates neuronal cells damage in a middle cerebral artery occlusion animal model. J Vet Med Sci 80: 676-683, 2018.
44. He GY, Yuan CG, Hao L, Xu Y and Zhang ZX: GBE50 attenuates inflammatory response by inhibiting the p38 MAPK and NF-κB pathways in LPS-stimulated microglial cells. Evid Based Complement Alternat Med 2014: 368598, 2014.
45. Skaper SD: Poly(ADP-ribosyl)ation enzyme-1 as a target for neuroprotection in acute central nervous system injury. Curr Drug Targets CNS Neurol Disord 2: 279-291, 2003.